

**Microneedle-assisted Dendritic Cell-targeted Nanoparticles  
for Transcutaneous DNA Immunization**

Journal:	<i>Polymer Chemistry</i>
Manuscript ID:	PY-ART-10-2014-001394.R1
Article Type:	Paper
Date Submitted by the Author:	28-Oct-2014
Complete List of Authors:	Hu, Ying; Zhejiang Pharmaceutical College, Xu, Beihua; College of Pharmaceutical Sciences, Zhejiang University, Xu, Jiaojiao; Zhejiang Pharmaceutical College, Shou, Dan; Department of Medicine, Zhejiang Academy of Traditional Chinese Medicine, Liu, Ergang; Shanghai Institute of Materia Medica, Chinese Academy of Sciences, Gao, Jian-Qing; Zhejiang University, Pharmaceutics Liang, Wenquan; Department of Pharmaceutics, College of Pharmaceutical Sciences, Zhejiang University, Huang, Yongzhuo; Shanghai Institute of Materia Medica, Chinese Academy of Sciences,

## ARTICLE

# Microneedle-assisted Dendritic Cell-targeted Nanoparticles for Transcutaneous DNA Immunization

Cite this: DOI: 10.1039/x0xx00000x

Received 00th January 2012, Accepted 00th January 2012  
Ying Hu,<sup>a,b</sup> Beihua Xu,<sup>a</sup> Jiaojiao Xu,<sup>a,c</sup> Dan Shou,<sup>d</sup> Ergang Liu,<sup>e</sup> Jianqing Gao,<sup>b</sup> Wenquan Liang,<sup>b</sup> and Yongzhuo Huang,<sup>\*e</sup>

DOI: 10.1039/x0xx00000x

[www.rsc.org/](http://www.rsc.org/)

Transcutaneous immunization (TCI) is an attractive vaccination strategy by targeting to the epidermal dendritic cells (DCs). TCI has been widely explored for protection against infectious diseases. Recently, its promising application in cancer immunotherapy has also attracted great attention. However, effective percutaneous delivery of the vaccines must overcome the formidable stratum corneum, as well as specifically target to DCs; both are big challenges. We developed the mannosylated grafted cell-penetrating peptide-low molecular weight PEI copolymer (CPP-PEI<sub>1800</sub>-Man) with combination of microneedle for DCs-targeting percutaneous delivery of DNA vaccine for malignant melanoma (MM) therapy. Mannose receptors are overexpressed on the surface of DCs. The microneedle-assisted in vivo skin penetration of the CPP-PEI<sub>1800</sub>-Man/DNA nanoparticles was investigated, and the DCs-targeting efficiency was measured. The induction of protective and therapeutic anti-tumor immunity by the CPP-PEI<sub>1800</sub>-Man/DNA nanoparticles was significantly enhanced, compared to the PEI<sub>25k</sub>/DNA vaccines. Transcutaneous vaccination with the microneedle-assisted CPP-PEI<sub>1800</sub>-Man/DNA efficiently promoted Trp<sub>2</sub>-specific cellular immune responses, resulting in effective protection against B16 melanoma challenge in BALB/c mice. Importantly, the CPP-PEI<sub>1800</sub>-Man/DNA nanoparticles strongly induced CD8<sup>+</sup> cytotoxic T lymphocyte activity and CD4<sup>+</sup> T cells that secreted the interferon- $\gamma$  and interleukin-12 cytokines against melanoma cells. As a result, cancer growth was inhibited and the survival time of B16-xenografted BALB/c mice prolonged. Therefore, the CPP-PEI<sub>1800</sub>-Man copolymer is promising for DC-specific vaccination, and the microneedle-assisted CPP-PEI<sub>1800</sub>-Man/DNA delivery represents a potential immunotherapeutic strategy for MM.

## Introduction

Malignant melanoma (MM) is an aggressive skin neoplasm featured by rapid tumor progression and metastasis, and is the most lethal skin cancer. MM is usually resistant to chemotherapy, leading to poor prognoses for the patients.<sup>1</sup> Evidence has shown that melanoma cells can be immunogenic, prompting extensive basic and clinical research in an attempt to develop effective anti-melanoma vaccines.<sup>2-4</sup> For example, tyrosinase-related protein 2 (Trp-2) is a melanogenic protease with overexpression in both melanocytes and melanomas, and has been used as a melanoma rejection antigen.<sup>5</sup> Immunization against TRP-2 can induce cytotoxic CD8<sup>+</sup> T cell responses.

The skin is highly immune reactive due to its unique immunological properties, in which there are abundant dendritic cells (DCs), typically the Langerhans cells (LCs), that can capture, process, and present foreign antigens (Ag) to

lymph nodes, and consequently prime effective immune responses.<sup>6, 7</sup> It thereby provides an ideal avenue for vaccination.

Transcutaneous immunization (TCI) has been an attractive vaccination strategy because it is non-invasive or minimally invasive, and can overcome the limitations of conventional vaccine immunization by intramuscular injection (IM), such as eliminating the need for the trained personnel and a cold chain for vaccine storage and transportation, the risk of needle reuse-related diseases, the fear and stress of children and parents.<sup>8, 9</sup> The epidermis is rich in LCs, thereby rendering it an ideal target site for vaccination. However, the stratum corneum, the top layer of the skin, acts as a physical barrier against vaccine penetration.<sup>10</sup> To improve percutaneous delivery of vaccines, microneedle-mediated TCI has been developed and represents a promising immunization modality for induction of strong immune responses. Furthermore, dose of antigen/vaccine can

be reduced because microneedle can effectively penetrate the stratum corneum and produce sufficiently micro-holes allowing for the transport of proteins and nanoparticles.<sup>11-14</sup> The first use of microneedle as a novel transcutaneous drug delivery system dated back to 1998.<sup>15</sup> Subsequently, the microneedle system has been applied in TCI for its effective delivery of various types of vaccines into the skin. For example, microneedle-mediated TCI with naked plasmid DNA could induce substantially stronger immune responses than hypodermic needle-based intramuscular injection of the same plasmid DNA.<sup>16</sup>

DCs are the target cells in TCI for vaccine delivery because they play an important role in primary immune activation. For targeted delivery of a non-viral gene vector to specific cells, receptor-mediated strategy is promising to achieve target specificity and avoid nonspecific interactions.<sup>17</sup> However, it still remains challenging for in vivo targeting delivery to epidemic DCs.

Mannose is a commonly used ligand that binds the cell-surface mannose receptors and triggers receptor-mediated endocytosis, and, consequently, increases intracellular delivery efficiency.<sup>18</sup> Mannose receptors are overexpressed on the surface of antigen-presenting cells, such as DCs and macrophages.

We previously demonstrated the feasibility of the mannosylated grafted polymeric vector for safe and efficient delivery of DNA in vitro.<sup>19</sup> In the present work, we further explored the in-vivo application of the mannosylated grafted cell-penetrating peptide-low molecular weight PEI copolymer (CPP-PEI<sub>1800</sub>-Man) for TCI, and the CPP-PEI<sub>1800</sub>-Man nanoparticles assisted by microneedle as a Trp-2 DNA vaccine delivery system for cancer immunotherapy (Scheme 1). CPP-PEI<sub>1800</sub>-Man was investigated for its targeted delivery to DCs in vivo. The efficiency of TCI with CPP-PEI<sub>1800</sub>-Man/DNA vaccine was measured and the immune priming and therapeutic efficacy in vivo was studied. Its possible mechanisms in cancer immunotherapy were also investigated.

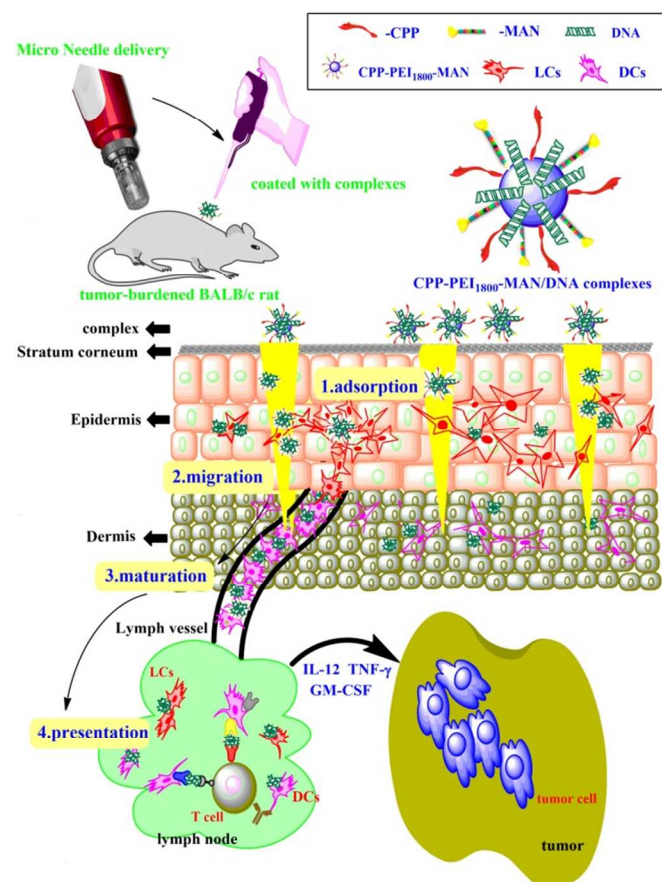
## Experimental section

### Materials

Branched PEI<sub>25k</sub>,  $\alpha$ -D-mannopyranosylphenylisothiocyanate (MPITC), N-succinimidy-3-(2-pyridyldithio) propionate (SPDP), and HEPES were purchased from Sigma-Aldrich (St. Louis, MO, USA). PEI<sub>1800</sub> was obtained from Alfa Aesar (Ward Hill, MA, USA). Cell-penetrating peptide (CPP; a sequence of TAT: RRRQRRKKRC-SH) were purchased from Shanghai Saiqi Co., Ltd. (Shanghai, China).

The plasmid pEGFP-N2 encoding enhanced green fluorescent protein (EGFP) was obtained from BD Biosciences/Clontech Co. (Mountain View, CA, USA) and was isolated and purified from DH5- $\alpha$  Escherichia coli using the Qiagen End-free Plasmid Purification Kit (Germantown, MD, USA) prior to use. The plasmid Trp2-GM-CSF-Fc-EGFP was constructed by our laboratory, which encoded the tumor antigen of the fused Trp-2 and GM-CSF (Granulocyte-macrophage colony-stimulating factor), with co-expression of EGFP marker. GM-CSF is an ideal vaccine adjuvant for inducing anti-tumor

immune responses, because it is a potent cytokine activator of DC antigen presentation, and actively participates in the initiation of danger signals for activating the immune system and eliciting tumor-specific responses. Its plausible mechanisms involving in cancer immunotherapy is that the GM-CSF secretion may recruit the DCs to migrate to the tumor and thus present antigens to T cells to generate a systemic, tumor-specific response.<sup>20</sup>

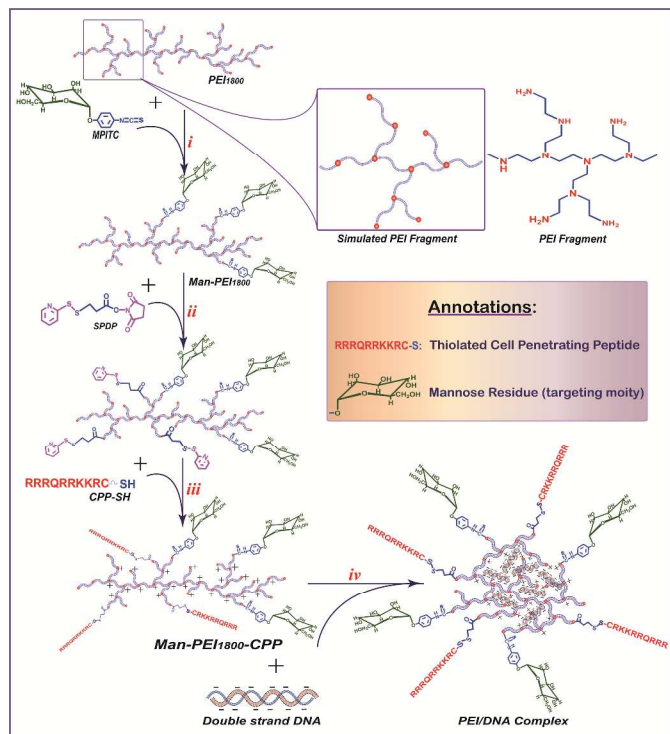


**Scheme 1.** Schematic diagram of microneedle-mediated transcutaneous delivery of CPP-PEI<sub>1800</sub>-Man/DNA nanocomplexes for anti-tumor immune treatment.

The plasmid pEGFP-N2, containing fused Trp<sub>2</sub>, and the GM-CSF and Fc genes, was prepared in a large scale using an endotoxin free kit (Qiagen). DNA concentrations were determined by measuring the UV absorbance at 260 nm. Carboxy-CdSe/ZnS quantum dots (QDs, water-soluble and green fluorescent) were purchased from Beijing Zhong Ke Wu Yuan Biotechnology Co., Ltd. (Beijing, China). Cell culture medium RPMI 1640 and fetal bovine serum were obtained from Life Technologies (Gibco, Carlsbad, CA, USA). Recombinant Trp<sub>2</sub> protein was purchased from R&D Systems (Minneapolis, MN, USA). Commercially available anti-CD4 and anti-CD8 immunohistochemistry kits (EnVision™) were obtained from DAKO Co. (Glostrup, Denmark). Interleukin (IL)-12 and Interferon (IFN)- $\gamma$  enzyme-linked immunosorbent assay (ELISA) kits, and PEI-labeled anti-mouse CD11c were purchased from Multi Sciences Biotech Co., Ltd. (Hangzhou, China). All other chemicals and solvents were obtained commercially and used without further purification.

### Synthesis and structural characterization of CPP-PEI<sub>1800</sub>-Man

The CPP-PEI<sub>1800</sub>-Man copolymer was synthesized via a three-step procedure.<sup>19</sup> First, mannose was conjugated to the PEI<sub>1800</sub> backbone via a reaction between the isothiocyanate group in MPITC and the amine group in PEI. Second, the mannosylated PEI was further activated using N-succinimidyl-3-(2-pyridyldithio) propionate (SPDP). Third, the thiolated CPPs were coupled to the activated mannosylated PEI, yielding a CPP-PEI<sub>1800</sub>-Man copolymer (Scheme 2).



**Scheme 2.** Preparation of CPP-PEI<sub>1800</sub>-Man (step i-iii) and PEI/DNA nanocomplexes (step iv).

### Preparation of complexes

The preparation and characterization was as described as the methods previously reported.<sup>19</sup> In brief, the PEI/DNA complexes were prepared at the desired N/P ratios of 10, as predetermined by the amounts of DNA and copolymer solutions. DNA solution was added to the PEI solution followed by gentle vortex for 10 s and further incubation at room temperature for 30 min. The zeta potential of the complexes was greater than 20 mV, measured by Malvern Nano ZS90. Moreover, Man-PEI<sub>1800</sub>-CPP was labelled by QDs as described previously.<sup>19</sup> The selection of QDs as a macromolecular tracking probe was based on the following reasons. First, the QDs are in nano scale, comparable to the macromolecular drugs in size. Second, the negatively charged QDs can bind with the polymeric carrier via electrostatic interaction, a drug-loading pattern similar to nucleic acid drugs.

### In vivo skin penetration study

For in vivo experiments, BALB/c mice (6–8 weeks old, 18–20 g) were purchased from the Ningbo University Animal Care

Center and housed in a standard specific pathogen-free environment. All animal experiments were performed in accordance with the protocols approved by the Ningbo University Animal Care and Use Committee. Twenty-four hours prior to the experiment, the hair on the abdominal skin was trimmed (an area of  $2 \times 2 \text{ cm}^2$ ). A microneedle array was applied onto the naked abdominal skin and maintained in the place for 2 min. After removal of the microneedle, the Man-PEI<sub>1800</sub>-CPP/QDs nanocomplex suspension was applied to the same region. After 1 h, the skin was thoroughly washed with saline. Skin samples from the treated areas were removed and processed by cryosection (7- $\mu\text{m}$  thick slices, Leica CM 1500 cryotome). The tissue slices contained epidermis, dermis, and skin appendages (including hair follicles, sweat glands, and sebaceous glands). These slices were observed using a confocal laser scanning microscope (CLSM; Olympus, FV-1000).

### In vivo targeting and migration assay

The Man-PEI<sub>1800</sub>-CPP/DNA complexes containing 50  $\mu\text{g}$  pEGFP-N2 in 100  $\mu\text{L}$  sterile PBS were topically applied onto the shaved skin with pretreatment of microneedle, and the efficacy of in vivo immunotherapy was monitored as described previously.<sup>21</sup> Cells from lymph nodes and spleens were dissected 36 h after immunization. Lymph nodes and spleen tissues were processed using a 100- $\mu\text{m}$  cell strainer and a syringe plunger. The tissue residues were rinsed with PBS and the cells were collected by centrifugation at 1000 rpm for 10 min at 4  $^{\circ}\text{C}$ . Red blood cell lysis buffer (3 mL) was added to the cells and the suspension was incubated for 3 min at room temperature. After centrifugation, the pelleted cells were washed three times with PBS and resuspended in complete culture medium (RPMI 1640 supplemented with 12 mM HEPES and 10% FBS). Splenocytes and lymph node cells were incubated with PEI-labeled anti-mouse CD11c antibody for 30 min at 4  $^{\circ}\text{C}$ , and then analyzed by flow cytometry as described previously,<sup>22</sup> and the dual-positive (GFP+/CD11c+) DCs were identified and measured.

### Tumor prevention experiment

For the tumor protection experiment, BALB/c mice (10 per group) were subjected to microneedle-assisted TCI as described above with the Man-PEI<sub>1800</sub>-CPP/DNA nanocomplexes containing 50  $\mu\text{g}$  pTrp<sub>2</sub>-GM-CSF-Fc-EGFP in 100  $\mu\text{L}$  sterile PBS for three times at weekly intervals. Control mice were topically treated with the naked DNA after microneedle application. One week after the third vaccination, mice were subcutaneously challenged in the right flank with B16 melanoma cells ( $2 \times 10^5$ ). The tumor progression was measured by its size and the survival curve was determined. Tumor size was determined by measuring the smallest (a) and largest (b) diameter by calliper. Tumor volume (V) was calculated using the formula as follow:

$$V = (a^2b)/2. \quad 23$$

### Assays to measure T cell responses

To detect Trp2-specific cellular immune responses, BALB/c mice (3 per group) were subjected to microneedle-assisted TCI with the PEI/pTrp2-GM-CSF-Fc-EGFP nanocomplexes at a dose of 50  $\mu\text{g}$  for three times at weekly intervals. At the experimental endpoint (two weeks after the third vaccination, the mice were euthanized, and splenocytes from the animals were cultured in 96-well plates in 100  $\mu\text{L}$  growth medium in the presence of 15  $\mu\text{g}\cdot\text{mL}^{-1}$  recombinant Trp<sub>2</sub> protein. After 72 h, the supernatants were collected and for determination of IFN- $\gamma$  and IL-12 by ELISA.

### Tumor treatment assay

To determine the therapeutic efficacy of various therapy regimens, mice bearing subcutaneous B16 melanoma (approximately 40 mm<sup>3</sup>) in the right flank were treated with the TCI procedures as described above. Each randomly-divided groups included 10 mice. The tumor volume was measured.

### Immunohistochemistry

Tumor tissues were collected and processed for immunohistochemical examination as described previously.<sup>24</sup> In brief, on day 21 after TCI, three mice from each experimental group were sacrificed. The tumors were dissected and processed for cryosection. The slices were washed twice for 5 min with PBS. After blocking with 0.1 mg·mL<sup>-1</sup> BSA, the slices were incubated with monoclonal anti-CD8 or anti-CD4 Ab at 4 °C overnight. The slices were then washed three times with PBS, followed by incubation with goat anti-mouse-IgG Fc horseradish peroxidase (HRP), and counterstaining with hematoxylin and eosin (H&E). Images were taken using a BX-51 microscope (Olympus, Japan).

### Statistical analysis

Data are reported as means  $\pm$  standard deviation (SD). Statistical analysis was performed using two-tailed Student t-test. Significant difference is represented as \* $P$ <0.05 and \*\*\* $P$ <0.01.

## Results

### In vivo trafficking assay

To observe the distribution of grafted-PEI/QD complexes in skin that was treated or not by the microneedle treatment, we used a water-soluble carboxyl CdSe/ZnS quantum dot (QD) as a probe, which can electrostatically bind with the graft-PEI copolymer.

Fluorescence was found mainly in the stratum corneum (Fig. 1, A & B) in the skin exposed to the CPP-PEI<sub>1800</sub>-Man/QD complexes without microneedle treatment or the naked QD with microneedle treatment. The skin penetration was improved by using microneedle-assisted PEI<sub>25k</sub>/QD complex, showing moderate fluorescence in the epidermal and dermal layers. By contrast, with pretreatment of microneedle, the CPP-PEI<sub>1800</sub>-Man/QD group displayed the strongest fluorescence activity in

the epidermal and dermal layers (Fig. 1, C & D), indicating its potential in transcutaneous delivery.

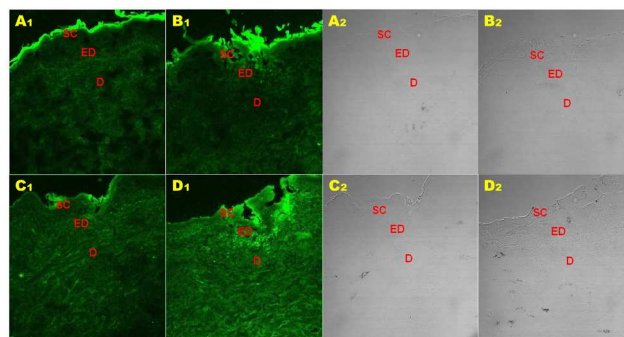


**Fig. 1** The distribution of QDs in the skins with different treatment. (A) the CPP-PEI<sub>1800</sub>-Man/QD complexes without microneedle pretreatment; (B) QD with microneedle pretreatment; (C) the PEI<sub>25k</sub>/QD complexes with microneedle pretreatment; (D) the CPP-PEI<sub>1800</sub>-Man/QD complexes with microneedle pretreatment, with the subscript number 1, or 2 represent fluorescent or bright field images, respectively. (SC, stratum corneum; ED, epidermis; D, dermis)

### In vivo studies of DC-targeting and migration

To determine whether the mannosylated graft-PEI delivery of DNA was able to target to the epidermal DCs, the plasmid pEGFP-N2 that encoded EGFP as a model DNA drug was used, which allowed the tracking of the biofate of the expressed EGFP. Splenocytes and lymph node cells were subjected to flow cytometry (Fig. 2). There was a higher ratio of CD11c+ DCs in the spleen and lymph nodes from the animals that received the microneedle-assisted administration of the CPP-PEI<sub>1800</sub>-Man/pEGFP-N2, compared to the control group. The percentage of dual-positive (GFP+/CD11c+) DCs in splenocytes and lymph node cells was 49.6% and 42.2%, respectively, displaying significant enhancement than those in the microneedle-assisted delivery of naked DNA or PEI<sub>25k</sub>/DNA group. This finding indicated that the CPP-PEI<sub>1800</sub>-Man copolymer can be used for DNA TCI, with aid of microneedle, for targeting to the draining lymphoid tissues (spleen and lymph node).

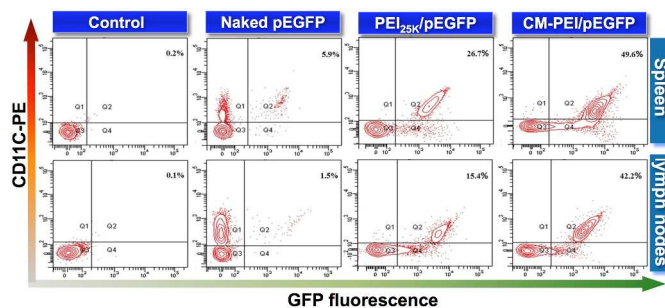


**Fig. 2** Flow cytometry assay of the dual-positive (GFP+/CD11c+) cells for evaluation of the in vivo targeting and migration of the DCs in mice challenged with different Pegfp-N2 formulations, with untreated mice served as control, and CM-PEI/pEGFP-N2 represents CPP-PEI<sub>1800</sub>-Man/pEGFP-N2.

### The induction of protective anti-tumor efficacy by TCI

To investigate the antitumoral immunity induced by the DC-targeted vaccine, the BALB/c mice were received TCI for three

times at weekly intervals. The mice were then challenged with tumor cells one week after the final immunization, and tumor development was monitored. TCI with the Man-PEI<sub>1800</sub>-CPP/pTrp<sub>2</sub>-GM-CSF-Fc-EGFP protected mice from B16 melanoma cell challenge, resulting in 90% survival of all mice during the experimental period (Fig. 3A). Furthermore, its inhibition rate of tumor growth was 68.5% at day 35 after challenge with tumor cells, with the tumor volume of 297.2 mm<sup>3</sup>. By contrast, that was 943.8 mm<sup>3</sup> for the PEI<sub>25k</sub>/pTrp<sub>2</sub>-GM-CSF-Fc-EGFP control group (Fig. 3B). It was observed that 30% of mice that received the CPP-PEI<sub>1800</sub>-Man/pTrp<sub>2</sub>-GM-CSF-Fc-EGFP vaccine could remain tumor-free for 14 days after B16 melanoma cell challenge, whereas only 10% in the group received the PEI<sub>25k</sub>-Man/pTrp<sub>2</sub>-GM-CSF-Fc-EGFP. Taking together, the CPP-PEI<sub>1800</sub>-Man/pTrp<sub>2</sub>-GM-CSF-Fc-EGFP vaccine significantly protected mice from challenge with B16 melanoma cells.

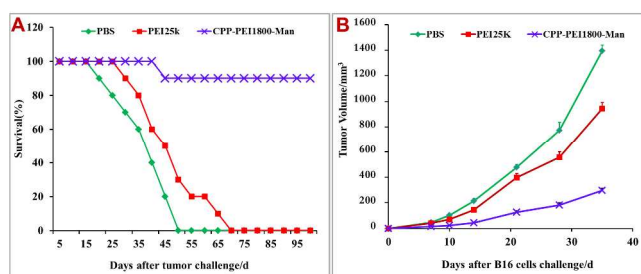


**Fig. 3.** The time-course of (A) survival time and (B) tumor volume change in the vaccinated mice following inoculation with B16 melanoma cells. Each data point represents the mean  $\pm$  SD;  $n = 10$ .

#### Determination of IFN- $\gamma$ and IL-12 cytokine levels

To quantify the extent of the immune responses induced by the Man-PEI<sub>1800</sub>-CPP/pTrp<sub>2</sub>-GM-CSF-Fc-EGFP complexes, the splenocytes isolated from the vaccinated mice were cultured in the presence of recombinant Trp<sub>2</sub> protein for 72 h. The IFN- $\gamma$  concentration in the splenocyte culture supernatants from the CPP-PEI<sub>1800</sub>-Man/DNA group was significantly higher (383 pg·mL<sup>-1</sup>) than that from the naked DNA control group (96 pg·mL<sup>-1</sup>) or the PEI<sub>25k</sub>/DNA group (184 pg·mL<sup>-1</sup>) (Fig. 4A). Similar trend was observed in the group receiving the CPP-PEI<sub>1800</sub>-Man/pTrp<sub>2</sub>-GM-CSF-Fc-EGFP, which produced significantly higher level of IL-12 (2953 pg·mL<sup>-1</sup>) than the non-DC-targeting groups (334 pg·mL<sup>-1</sup> for the naked DNA and 1185 pg·mL<sup>-1</sup> for PEI<sub>25k</sub>/DNA group) (Fig. 4B).

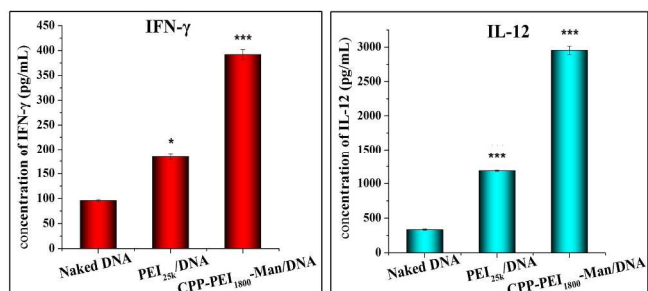


**Fig. 4.** Cytokine concentrations of (A) IFN- $\gamma$  and (B) IL-12 in the supernatant of the cultured splenocytes. Each data point represents the mean  $\pm$  SD;  $n = 3$ ; \*\*\* $P < 0.01$  and \* $P < 0.05$ .

#### Therapeutic efficacy

The therapeutic effect of TCI was tested in the mice with xenografted melanoma. The CPP-PEI<sub>1800</sub>-Man/pTrp<sub>2</sub>-GM-CSF-Fc-EGFP vaccination induced significant therapeutic anti-tumor immunity, with prolonged survival time (Fig. 5A). The tumor growth inhibition rate was 48%. Its mean tumor volume was measured to be 594.3 mm<sup>3</sup>, while that was 1143.3 mm<sup>3</sup> in the PEI<sub>25k</sub>/pTrp<sub>2</sub>-GM-CSF-Fc-EGFP control group (Fig. 5B). These results suggested that microneedle assisted TCI with the DC-targeting vaccine delivery significantly enhanced the therapeutic efficacy compared to the non-DC targeting method.

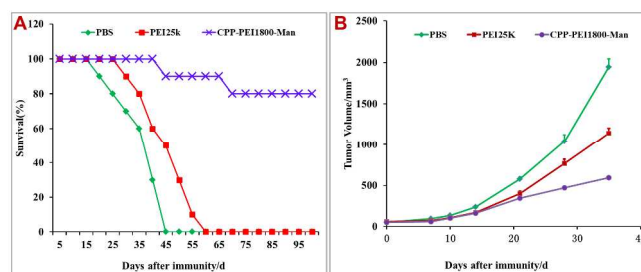


**Fig. 5.** Treatment efficacy represented by the time-course of (A) survival time and (B) tumor volume change in mice bearing tumors. Each data point represents the mean  $\pm$  SD;  $n = 10$ .

#### Immunohistochemical examination

The occurrence of necrosis and apoptosis was examined using H&E staining. Lymphocyte infiltration was observed in tumor tissues in the vaccinated mice (Fig. 6). The tumor-infiltrating lymphocytes were markedly increased in the CPP-PEI<sub>1800</sub>-Man/pTrp<sub>2</sub>-GM-CSF-Fc-EGFP group, compared to the other groups (Fig. 6). Trp-2-induced anti-tumor immunity is required the activation of CD8<sup>+</sup> T cells, and the cytotoxic CD8<sup>+</sup> T cell responses are dependent on CD4<sup>+</sup> T cell help.<sup>25</sup> In tumor slices, there were greater numbers of CD8<sup>+</sup> and CD4<sup>+</sup> T cells detected in the CPP-PEI<sub>1800</sub>-Man/pTrp<sub>2</sub>-GM-CSF-Fc-EGFP group than any other groups, indicating that the enhanced T cell-mediated antitumor immunity.

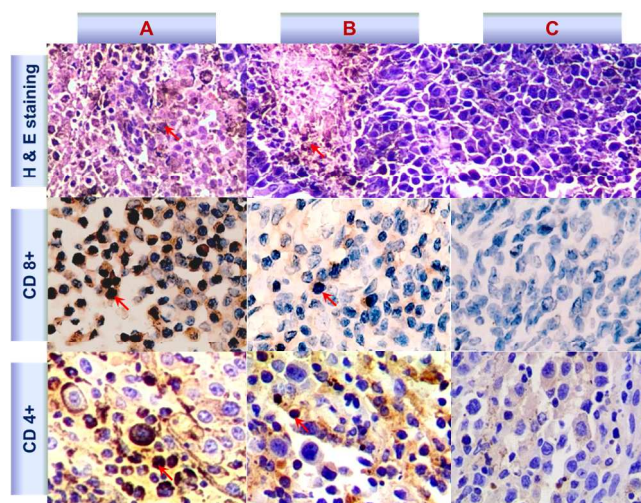


**Fig. 6.** Immunohistochemical examination of tumor slices from the groups of (A) Man-PEI<sub>1800</sub>-CPP/pTrp<sub>2</sub>-GM-CSF-Fc-EGFP, (B) PEI<sub>25k</sub>/pTrp<sub>2</sub>-GM-CSF-Fc-EGFP, and (C) CPP-PEI<sub>1800</sub>-Man/pTrp<sub>2</sub>-GM-CSF-Fc-EGFP.

Fc-EGFP, and (C) naked pTrp<sub>2</sub>-GM-CSF-Fc-EGFP (original magnification, × 200; T cells are marked by arrows).

## Discussion

DNA vaccination is an attractive therapeutic approach by inducing anti-tumor immunity.<sup>26</sup> The general approach involves the use of immunogenic genes that encode tumor-associated antigens presented by major histocompatibility complex (MHC) class I molecules for priming CD8<sup>+</sup> cytotoxic T lymphocytes (CTLs). However, in non-human primates and human volunteers, optimal antibody and CTL responses were only induced by high doses of DNA.<sup>27, 28</sup> Therefore, it is necessary to investigate novel methods to improve the immunogenicity of the DNA vaccines. Various strategies, such as vector modification, adjuvants, and efficient DNA delivery, have been explored. To improve the efficiency of DNA delivery, two major issues should be considered: (1) targeting delivery of DNA to some specific type of cells (e.g., DCs), and (2) improved cellular uptake.<sup>29</sup> Targeted activation of DCs is an important method related to the development of cancer vaccines because these cells play a pivotal role in elicitation of anti-tumor immunity.<sup>30</sup>

Our strategy was featured by the mannose-mediated epidermal DC-targeting delivery and CPP-PEI<sub>1800</sub> copolymer-mediated gene transfection. The Man-PEI<sub>1800</sub>-CPP/DNA complexes could target to and enter the DCs, which then migrated into the lymph nodes with expression of the tumor-associated antigens. The Man-PEI<sub>1800</sub>-CPP carries additional benefits. For example, the low molecular weight PEI is biocompatible and low cytotoxic, which can bind and condense DNA, and CPP could facilitate cellular uptake of DNA.

Induction of adaptive T cell immune responses is important for effective immunotherapy, represented by enhanced secretion of cytokines, such as IFN- $\gamma$ , IL-4, or IL-12. Our results showed that CTLs primed by the Man-PEI<sub>1800</sub>-CPP/pTrp<sub>2</sub>-GM-CSF-Fc-EGFP yielded high levels of IFN- $\gamma$  and IL-12, which are the key cytokines that promote Th1 cell differentiation. Large number of CD4<sup>+</sup> and CD8<sup>+</sup> T cells was found to infiltrate the solid tumors as a consequence of TCI. Moreover, CD4<sup>+</sup> and CD8<sup>+</sup> T cells can promote and amplify immune responses through the secretion of cytokines, such as IFN- $\gamma$ .<sup>31</sup>

The Man-PEI<sub>1800</sub>-CPP/DNA nanoparticles could induce antigen-specific cellular immune responses, primarily, the Th1 cell responses. Cellular immune responses were responsible for protection against tumor challenge. Moreover, they also remarkably arrested the growth of the established tumor.

## Conclusion

In summary, we developed a novel DNA vaccine transcutaneous delivery system based on the DC-targeting Man-PEI<sub>1800</sub>-CPP copolymer. By combination with microneedle, this epidermal DC-targeting DNA vaccine delivery successfully elicited both protective and therapeutic immune responses. The mechanism of antitumor activity was probably based on the recruitment of CD4<sup>+</sup> and CD8<sup>+</sup> T cells

and the induction of IFN- $\gamma$  and IL-12 cytokine production. This represented a promising TCI strategy with DC-targeting DNA delivery for inducing cellular immune responses for cancer immunotherapy.

## Acknowledgements

This study was supported by the Natural Science Foundation of China (NSFC 30973648, 81422048), and the Natural Science Foundation of Zhejiang Province, China (Grant No. LY12H30002, Z14H300001).

**Keywords:** microneedle, melanoma, transcutaneous immunization, dendritic cells, DNA vaccine, tyrosinase-related protein 2

## Notes and references

- <sup>a</sup> Zhejiang Pharmaceutical College, Ningbo, Zhejiang, China  
<sup>b</sup> College of Pharmaceutical Sciences, Zhejiang University, Hangzhou, Zhejiang, China  
<sup>c</sup> Department of Medicine, Wenzhou Medical University, Wenzhou, Zhejiang, China  
<sup>d</sup> Department of Medicine, Zhejiang Academy of Traditional Chinese Medicine, Hangzhou, Zhejiang, China  
<sup>e</sup> Shanghai Institute of Materia Medica, Chinese Academy of Sciences, 501 Hai-ke Rd, Shanghai 201203, China. Email: [yzhuang@simm.ac.cn](mailto:yzhuang@simm.ac.cn); Fax: +86 21 2023-1981; Tel: +86 21 2023-1000 ext. 1401

† Electronic Supplementary Information (ESI) available: See DOI: 10.1039/b000000x/

- J. Eberle, B. M. Kurbanov, A. M. Hossini, U. Trefzer and L. F. Fecker, *Drug resistance updates : reviews and commentaries in antimicrobial and anticancer chemotherapy*, 2007, **10**, 218-234.
- L. Fang, A. S. Lonsdorf and S. T. Hwang, *J Invest Dermatol*, 2008, **128**, 2596-2605.
- T. Tuting, *Pigment Cell Melanoma Res*, 2013, **26**, 441-456.
- S. L. Topalian, G. J. Weiner and D. M. Pardoll, *J Clin Oncol*, 2011, **29**, 4828-4836.
- M. C. Balcos, S. Y. Kim, H. S. Jeong, H. Y. Yun, K. J. Baek, N. S. Kwon, K. C. Park and D. S. Kim, *Acta Pharmacol Sin*, 2014, **35**, 489-495.
- C. DeBenedictis, S. Joubert, G. Zhang, M. Barria and R. F. Ghohestani, *Clinics in dermatology*, 2001, **19**, 573-585.
- K. Sugita, K. Kabashima, K. Atarashi, T. Shimauchi, M. Kobayashi and Y. Tokura, *Clin Exp Immunol*, 2007, **147**, 176-183.
- K. Matsuo, Y. Yokota, Y. Zhai, Y. S. Quan, F. Kamiyama, Y. Mukai, N. Okada and S. Nakagawa, *J Control Release*, 2012, **161**, 10-17.
- S. M. Bal, Z. Ding, E. van Riet, W. Jiskoot and J. A. Bouwstra, *J Control Release*, 2010, **148**, 266-282.
- A. Naik, Y. N. Kalia and R. H. Guy, *Pharmaceutical science & technology today*, 2000, **3**, 318-326.
- J. A. Matriano, M. Cormier, J. Johnson, W. A. Young, M. Buttery, K. Nyam and P. E. Daddona, *Pharm Res*, 2002, **19**, 63-70.

12. M. R. Prausnitz, *Advanced drug delivery reviews*, 2004, **56**, 581-587.
13. G. Li, A. Badkar, S. Nema, C. S. Kolli and A. K. Banga, *Int J Pharm*, 2009, **368**, 109-115.
14. W. Z. Li, M. R. Huo, J. P. Zhou, Y. Q. Zhou, B. H. Hao, T. Liu and Y. Zhang, *Int J Pharm*, 2010, **389**, 122-129.
15. S. Henry, D. V. McAllister, M. G. Allen and M. R. Prausnitz, *J Pharm Sci*, 1998, **87**, 922-925.
16. J. A. Mikszta, J. B. Alarcon, J. M. Brittingham, D. E. Sutter, R. J. Pettis and N. G. Harvey, *Nat Med*, 2002, **8**, 415-419.
17. B. Xiao, X. Wang, Z. Qiu, J. Ma, L. Zhou, Y. Wan and S. Zhang, *J Biomed Mater Res A*, 2013, **101**, 1888-1897.
18. S. S. Diebold, M. Kursa, E. Wagner, M. Cotten and M. Zenke, *J Biol Chem*, 1999, **274**, 19087-19094.
19. Y. Hu, B. Xu, Q. Ji, D. Shou, X. Sun, J. Xu, J. Gao and W. Liang, *Biomaterials*, 2014, **35**, 4236-4246.
20. I. Borrello and D. Pardoll, *Cytokine Growth Factor Rev*, 2002, **13**, 185-193.
21. Z. Ding, F. J. Verbaan, M. Bivas-Benita, L. Bungener, A. Huckriede, D. J. van den Berg, G. Kersten and J. A. Bouwstra, *J Control Release*, 2009, **136**, 71-78.
22. H. Wei, S. Wang, D. Zhang, S. Hou, W. Qian, B. Li, H. Guo, G. Kou, J. He, H. Wang and Y. Guo, *Clin Cancer Res*, 2009, **15**, 4612-4621.
23. Y. Li, J. Subjeck, G. Yang, E. Repasky and X. Y. Wang, *Vaccine*, 2006, **24**, 5360-5370.
24. S. A. Chen, M. H. Tsai, F. T. Wu, A. Hsiang, Y. L. Chen, H. Y. Lei, T. S. Tzai, H. W. Leung, Y. T. Jin, C. L. Hsieh, L. H. Hwang and M. D. Lai, *Clin Cancer Res*, 2000, **6**, 4381-4388.
25. A. N. Houghton, J. S. Gold and N. E. Blachere, *Curr Opin Immunol*, 2001, **13**, 134-140.
26. J. Rice, C. H. Ottensmeier and F. K. Stevenson, *Nature reviews. Cancer*, 2008, **8**, 108-120.
27. S. Calarota, G. Bratt, S. Nordlund, J. Hinkula, A. C. Leandersson, E. Sandstrom and B. Wahren, *Lancet*, 1998, **351**, 1320-1325.
28. R. Wang, D. L. Doolan, T. P. Le, R. C. Hedstrom, K. M. Coonan, Y. Charoenvit, T. R. Jones, P. Hobart, M. Margalith, J. Ng, W. R. Weiss, M. Sedegah, C. de Taisne, J. A. Norman and S. L. Hoffman, *Science*, 1998, **282**, 476-480.
29. G. Otten, M. Schaefer, B. Doe, H. Liu, I. Srivastava, J. zur Megede, D. O'Hagan, J. Donnelly, G. Widera, D. Rabussay, M. G. Lewis, S. Barnett and J. B. Ulmer, *Vaccine*, 2004, **22**, 2489-2493.
30. S. H. Seo, H. T. Jin, S. H. Park, J. I. Youn and Y. C. Sung, *Vaccine*, 2009, **27**, 5906-5912.
31. J. Zhang, H. Tian, C. Li, L. Cheng, S. Zhang, X. Zhang, R. Wang, F. Xu, L. Dai, G. Shi, X. Chen, Y. Li, T. Du, J. Deng, Y. Liu, Y. Yang, Y. Wei and H. Deng, *Mol Immunol*, 2013, **55**, 264-274.